Journal of Constructional Steel Research 70 (2012) 308–316

Contents lists available at SciVerse ScienceDirect

Journal of Constructional Steel Research

Experimental investigation on cyclic behavior of perforated steel plate shear walls

H. Valizadeh, M. Sheidaii *, H. Showkati

Civil Engineering Department, Urmia University, Urmia, Iran

ARTICLE INFO

Article history:
Received 16 March 2011
Accepted 30 September 2011
Available online 4 November 2011

Keywords:
Steel plate shear wall
Opening
Elastic stiffness
Shear strength
Ductility
Energy absorption

ABSTRACT

In recent decades, steel plate shear walls have come to be considered as a convenient system for resisting lateral loads due to earthquakes and wind, especially in tall buildings, because of their ductile and energy absorption behaviors. The existence of openings affects the seismic behavior and performance of steel plate shear walls. In the present research, the effects of opening dimensions as well as slenderness factors of plates on the seismic behavior of steel plate shear walls are studied experimentally. Eight 1:6 scaled test specimens, with two plate thicknesses and four different circular opening ratios at the center of the panel, have been manufactured and were tested under the effects of cyclic hysteresis loading at the thin-walled structures research laboratory of Urmia University, Urmia, Iran. The hole was put in the center of the panel because this is the most detrimental location in view of the panel tension field action. The obtained results signify a stable and desired behavior of steel plate shear walls for large displacements of up to 6% drift. The creation of openings decreases the initial stiffness and strength of the system, and increasing the opening diameter will intensify this matter. The obtained ductility of specimens shows the stable functioning of a system in the nonlinear range. Although the stable cyclic behavior of specimens in the nonlinear range causes mostly a dissipation of energy during the loading of samples, but existence of an opening at the center of the panel causes a noticeable decrease in energy absorption of the system.

1. Introduction

Over the last decade, a widespread interest has been shown in the application of steel plate shear walls ($SPSW_s$)[1] as a desirable resistant system against the lateral load in buildings. A steel plate shear wall is similar to a plate girder that is placed vertically and is expanded in the total height of the building. High elastic stiffness, high ductility and stable hysteresis loops are some of the desirable characteristics of an SPW system. Because of the dissipation of a large amount of energy, steel plate shear walls can be beneficial in highly active seismic zones.

In comparison with reinforced concrete walls, an SPW system shows a high capacity for energy absorption with stable hysteresis behavior and diagonal tensile field action of the web. In addition, SPW systems are lighter than concrete walls. For these reasons, an SPW system will lead to a reduction in the earthquake force. By using shop-welded, field-bolted SPWs, field inspection is improved and a high level of quality control can be achieved. For architects, the increased versatility and space saving because of the smaller cross-section of SPWs, compared to reinforced concrete shear walls, is a distinct benefit, especially in high-rise buildings, where reinforced concrete shear walls in lower floors become very thick and occupy a large proportion of the floor plan [1].

In some cases, the existence of openings is inevitable because of architectural reasons, passing equipment, or structural reasons, such as ductility and rigidity control. Therefore, it is necessary to do research on the effects of openings on the seismic behavior of steel plate shear walls.

To study the load–displacement characteristics of SPWs, Sabouri-Ghomi and Roberts carried out a series of cyclic quasi-static tests in 1991 on 16 unreinforced thin panels, some of which had openings, at small scales [2,3]. The frame had hinge joints, and the plate was connected to boundary members by bolts. The loading and unloading operations were carried out along the diagonals for creating pure shear. All of the panels showed adequate ductility and a capability for dissipating a large amount of energy. They also presented a theoretical method for calculating the shear capacity of the steel plate shear walls, named the Plate and Frame Interaction (PFI) method. Studying the experimental perforated specimens, Sabouri and Roberts proposed an empirical factor $(1-D/d)$ for the decreasing strength and stiffness of steel plate shear walls due to the existence of openings, where D is the opening diameter and d is the panel height.

In 2000, Deylami and Daftari analyzed more than 50 models with a rectangular opening in the center of the panel using a NISA Π nonlinear finite element program. They investigated the effects of some important geometric parameters, such as sheet thickness, the ratio of opening height to width, and the areal percentage of the opening [4]. In cases of small opening percentages, the decrease in shear capacity was more dependent on the plate thickness. The ratio of

* Corresponding author. Tel.: +98 441 2972865; fax: +98 441 2773591.
E-mail address: m.sheidaii@urmia.ac.ir (M. Sheidaii).

[1] Or steel plate walls (SPW_s).

0143-974X/$ – see front matter © 2011 Elsevier Ltd. All rights reserved.
doi:10.1016/j.jcsr.2011.09.016

height to optimized width of the opening has been a function of the plate thickness, and it has not been dependent on the opening percentage. In thinner steel plate shear walls, the maximum shear capacity has been achieved by a smaller ratio of height to width of the opening. Also, the decrease in shear capacity after reaching a maximum amount has been slower in thick plates than in thin plates. In all cases, the optimized shear capacity is achieved when the ratio of height to width of the openings is greater than 1.

In 2004, Vian and Bruneau from the University at Buffalo began a joint experimental study on SPWs with National Taiwan University [5]. Three single-story steel panel shear wall specimens were tested. The specimens utilized low yield strength steel infill panels and reduced beam sections at the beam ends. The first specimen had a solid panel, the second one had 20 openings with diameters of 200 mm and the third specimen had quarter-circle cutouts in the panel corner, which were reinforced to transfer the panel forces to the adjacent framing. In this research all specimens were tested under cyclic quasi-static loading according to the ATC-24 protocol [6]. The results of these experiments indicate that steel plate shear walls with low yield strengths can be considered as a practical choice for resistance against lateral loads during earthquakes. Utilizing a thin panel with small yield strength will cause a decrease in the strength and quick start of energy dissipation by the panel. The panels with openings show a decrease in strength and stiffness, so they may be used when steel plates with small yield strength are not readily available.

Kharrazi et al. [7] have proposed a theoretical model named Modified Plate and Frame Interaction (M-PFI) for the shear and bending analysis of ductile steel plate shear walls. In this model, the behavior of steel plate shear walls was divided into three different parts: elastic buckling, post buckling, and yielding. Considering the interaction between shear and flexural behavior of steel shear walls, the M-PFI model describes the behavior of SPW systems, and a good compatibility with different experimental results is accessible.

By studying the previous work on steel plates shear walls, it seems that, despite the inevitable reasons for existing openings in SPW systems, few researchers have studied the effects of openings on the seismic behavior of SPWs. In this research, to study the effect of slenderness factor, opening ratio and the failure modes of steel plate shear walls, eight specimens were designed to 1:6 scale and subjected to cyclic loading. The hole is put in the center of panel because this is the most detrimental location in view of the panel tension field action. The primary parameters of initial stiffness, shear strength, ductility and energy dissipation rate were determined.

2. Analytical formulas for shear force-displacement

The results obtained from experimental specimens can be investigated by M-PFI formulas proposed for calculating the critical buckling and yielding capacity [7]. Because of the hinged beam column joints of the laboratory frame, the frame system does not provide any considerable resistance against lateral forces. Thus, the panel strength against lateral forces only includes the strength of the infill plate. A diagram of shear force-displacement related to a steel plate with dimensions of b, d and a thickness of t is given in Fig. 1. Points C and D in Fig. 1 indicate the buckling and yielding points of the steel plate, respectively.

2.1. Buckling stage

The critical buckling shear stress, τ_{cr}, for a steel plate is calculated as follows [8]:

$$\tau_{cr} = \frac{k\pi^2 E}{12(1-\mu^2)}\left(\frac{t}{b}\right)^2 \le \tau_y = \frac{\sigma_0}{\sqrt{3}} \tag{1}$$

where t, b, E, μ, τ_Y and σ_0 are the thickness of the steel plate, width of the steel plate, elasticity modulus, Poisson's ratio, shear yielding stress and uniaxial yielding stress of the plate, respectively. The shear buckling factor k depends on the steel plate aspect ratio and boundary conditions, it is equal to 9.35 for a simple supported square plate.

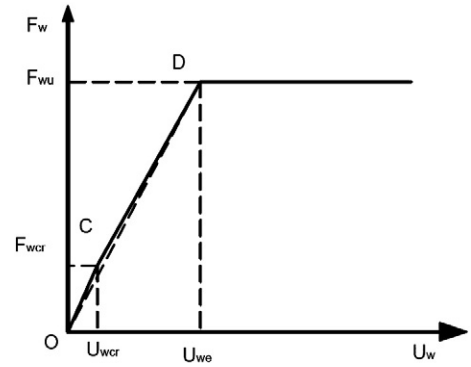

Fig. 1. Shear force-displacement diagram of a steel plate with sufficient supports only [1].

Thus, the critical shear force, F_{cr}, and critical shear displacement, U_{cr}, of a plate can be calculated by:

$$F_{cr} = \tau_{cr}\, b\, t \tag{2}$$

$$U_{cr} = \frac{\tau_{cr}}{G}\, d \tag{3}$$

where G and d are the shear modulus of the steel plate's materials and height of the steel plate, respectively. By calculating F_{cr} and U_{cr} using Eqs. (2) and (3), the position of point C will be specified in the shear force-displacement diagram of Fig. 1.

2.2. Post-buckling stage

It is assumed that in the post-buckling stage, the diagonal tension field will expand with an angle θ from the horizon throughout the entire web plate. By calculating the total stress of the plate at the time of yielding according to the Von Mises yield criterion for thin plates, the shear strength of the web plate, F_u, can be specified as follows [7]:

$$F_u = \left(\tau_{cr} + \frac{1}{2}\sigma_{ty}\sin 2\theta\right) b\, t \tag{4}$$

where σ_{ty} is the stress of the tension field in yielding time.

The limiting elastic shear displacement, U_e, is given as [7]:

$$U_e = \left(\frac{\tau_{cr}}{G} + \frac{2\sigma_{ty}}{E\sin 2\theta}\right) d \tag{5}$$

To further simplify the calculations of the shear load displacement diagram, lines OC and CD in Fig. 1 can be substituted by a straight line OD.

Roberts and Sabouri concluded that the strength and stiffness linearly decreases with the increases in $(1-D/d)$, where D is the opening diameter and d is the panel height [3]. The reduction factors proposed by Roberts and Sabouri were used in the aforementioned formulas for considering the strength and stiffness decrease in perforated specimens in the present study.

3. Test program

For studying the effect of the slenderness factor and opening dimension on the seismic parameters of steel plate shear walls, eight 1:6 scale specimens were prepared and tested under cyclic loading in the thin-walled structure research laboratory of Urmia University. The details of the testing hinge frame, preparation of specimens and loading process are given below.

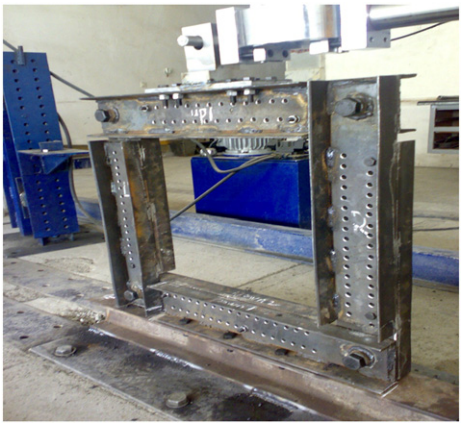

Fig. 2. Hinge frame before placing infill plate [9].

3.1. Hinge frame

For reducing behavioral complexity due to frame and steel plate interaction under lateral loading, a hinge frame with a high safety factor has been designed and fabricated. The centerline to centerline spacing between the 2U120 DIN1026 beams and columns of the fabricated frame was 620 mm. Considering the height of the applied channel sections for the framing system, the dimensions of the internal plates were 500 × 500 mm. For strengthening and rigid action of the beams and columns, in addition to preventing bearing failure in the web of the boundary members, a border plate of thickness 8 mm was connected to the channels web by a fillet weld. For providing a hinged connection, the beams and columns were connected with only a 24 mm diameter ASTM A490 bolt, as shown in Fig. 2. For connecting the steel plate inside the frame, two rows of 10 mm diameter ASTM A490 bolts were used for each frame member (Fig. 3).

3.2. Experimental specimens

Experimental specimens, as listed in Table 1, have been considered to study the seismic behavior of steel plate shear walls experimentally. To ignore the frame effect in tolerating the lateral force and its relevant complexity, the connection between boundary members has been considered as a hinged joint. The variables considered in these specimens were the slenderness factor (plate width to thickness ratio) and the opening ratio (opening diagonal to plate height ratio). To this end, two thicknesses of 0.37 and 0.7 mm were selected for the plates. For each thickness, a panel without any opening and three panels with circular openings of diameters 100, 175 and 250 mm have been tested. To specify the material properties of the steel plates, four tension test coupons have been prepared and tested according to the ASTM A370-97a 2001 standard [10]. A summary of the tests results are presented in Table 2.

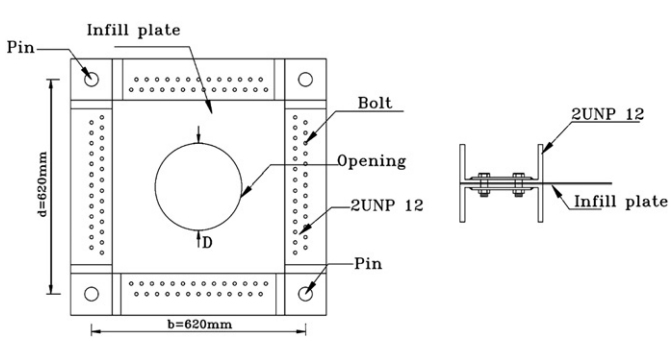

Fig. 3. Specifications and dimensions of the frame and details of the plate connection to the boundary members of the SPW specimen.

Table 1
Specifications of experimental specimens.

	Specimen	Plate thickness (mm)	Slenderness factor	Opening diagonal (mm)	Opening ratio
First series	SPW1	0.7	715	0	0
	SPW2	0.7	715	100	0.2
	SPW3	0.7	715	175	0.35
	SPW4	0.7	715	250	0.5
Second series	SPW5	0.37	1350	0	0
	SPW6	0.37	1350	100	0.2
	SPW7	0.37	1350	175	0.35
	SPW8	0.37	1350	250	0.5

3.3. Loading and boundary condition

After adjusting the internal steel plate and establishing the system on the rigid base of the laboratory, the hinge of the upper beam was installed and connected to the loading hydraulic jack by a load cell, as shown in Fig. 4. As can be seen in Fig. 5, three transducers have been used for the measuring cyclic displacement of the structure and controlling support settlement. For calculating the strain amount during loading for unperforated specimens, two strain gauges on the main diagonal and one strain gauge on the secondary diagonal in each loading direction were used (Fig. 5).

For perforated specimens, one strain gauge for each main and secondary diagonal in each loading direction (four strain gauges in total) has been used. In real buildings, lateral bracing at the ceiling level is created by a slab. To emulate this, the specimen was braced laterally as shown in Fig. 6. To study the seismic behavior of the specimens, a cyclic loading process has been defined in five cycles up to a drift of 6% (Fig. 7). The first cycle had a drift of 0.5% in the linear range for considering the conditioning situations, and the next four cycles considered were in the nonlinear range of the system seismic behavior. Loading was done at a low speed to prevent a dynamic mode.

4. Discussion of results

It has been observed that the producing sound and impact at the moment of plate buckling will decrease by placing an opening in a panel. This will be totally removed in specimens with the largest opening ratio. The displacement and expansion of the tension field in our experimental specimens is given in Fig. 8. The inclination angle of the tension field is 45° because all of the experimental specimens were square in shape. Expansion of the tension field and buckling waves began with one wave on the main diagonal and then, by increasing the lateral displacement of the specimen, second waves along the same direction as the main wave were formed. Buckling wave formation in the plate is more evident in plates with lesser thicknesses, and it is easier to distinguish the waves. As shown in Fig. 8a, five complete

Table 2
Specified characteristics of the materials by tension test.

Specimen	Specimen thickness (mm)	Yielding stress (N/mm²)	Ultimate stress (N/mm²)
Sheet 1	0.70	180	300
Sheet 2	0.70	180	300
Sheet 3	0.37	299	375
Sheet 4	0.37	299	375

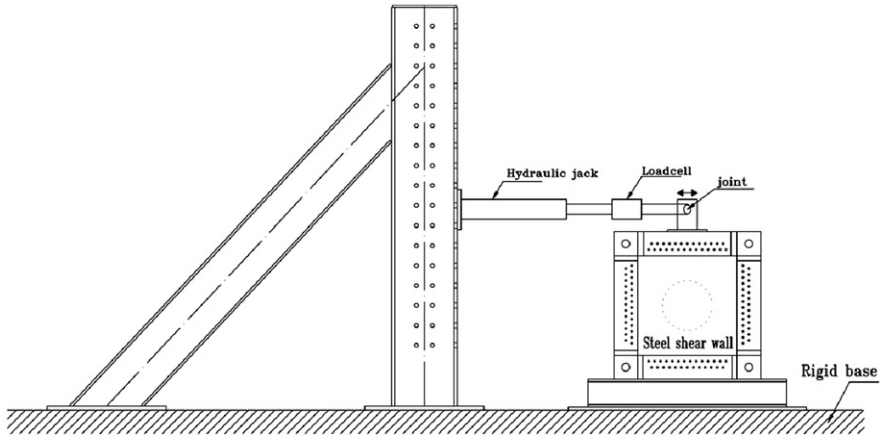

Fig. 4. Set up of specimen in the laboratory.

waves were seen for the specimen without an opening and a plate thickness of 0.7 mm (SPW1) in 4.5% drift. For the specimen without an opening and a plate thickness of 0.37 mm (SPW5) in 3% drift, seven complete waves with a 45° angle were observed (Fig. 8e). Due to their higher ultimate strength, specimens without an opening have shown a bearing failure of the plate and bolts in connections at the end of test program (Fig. 9). In perforated specimens with less plate thickness (SPW7 and SPW6), plate tearing failure occurred around the opening due to stress concentration (Fig. 10). The force-displacement hysteresis loops along with theoretical results for the experimental specimens are given in Fig. 11. Placing an opening at the center of the panel decreases initial stiffness and lateral resistance capacity of the steel plate shear wall systems. With an increase in the opening diameter, the decrease of strength and initial stiffness will be more intensive.

4.1. Elastic stiffness and strength

The behavior of thin steel plate shear walls is affected by tension field action and is controlled by boundary conditions. In steel plate shear walls with a bolted connection between plate and boundary members, slippage in the bolted connection and plate yielding adjacent to the boundary will decrease the wall's stiffness more than a welded connection [11]. Therefore, a steel plate shear wall with such a bolted connection will have a smaller amount of elastic stiffness. Due to slipping of the connection and local deformations, its initial yielding will happen under a smaller load [11]. In the prepared experimental specimens, the connection between plate and boundary members was considered to be a bolted connection. Checking the connection at the end of testing has shown the crippling failure of the bolt holes in high drifts, especially at the edges and in the same direction as the diagonal tension field (Fig. 9). This failure was accompanied with tear lines along with bolts (Fig. 9). Crippling will expand at connection points before the achievement of force at the limit that produces a diagonal tension field and plate yielding expansion. A summary of the results in the laboratory and theoretical formulations for the specimens is shown in Table 3. As can be seen in this table, the used analytical method has been estimated the ultimate shear strength of the experimental specimens conservatively. But, this method overestimates the initial stiffness because of the slippage in bolted connections. A comparison of the results achieved from the analyses and the envelope of the force-displacement hysteresis diagram for the SPW8 specimen is shown in Fig. 12. As mentioned before, the main reasons for differences between the initial stiffness of a specimen and the analytical results are bolt slippage and geometric imperfections of the experimental specimens [12]. The main reason for differences in the strength amounts is that the material hardening was not considered in a theoretical way. According to the different failure modes of specimens, the amount of force corresponding to 3% drift has been selected and compared (Table 4) for studying the effect of opening dimension on panel strength.

4.2. Ductility

Several tests conducted on the steel shear walls showed that the system has a good ductility. According to tests carried out at the University of Alberta, the behavior factor of steel plate shear walls has been estimated to be more than 2.5 times the conventional moment

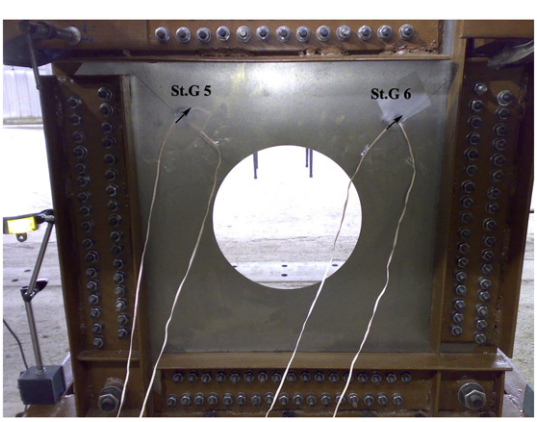

Fig. 5. Installation place of the transducers and the strain gauges in the SPW1 specimen.

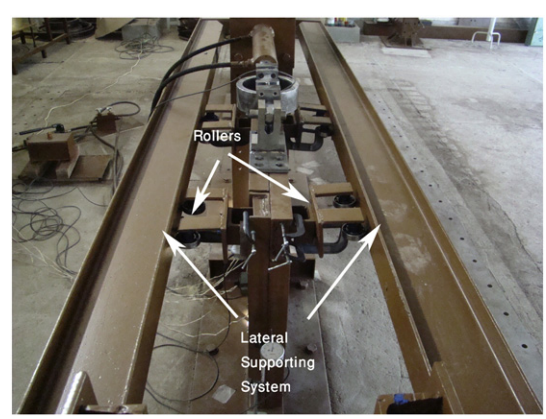

Fig. 6. Lateral bracing system of the SPW specimen in the laboratory.

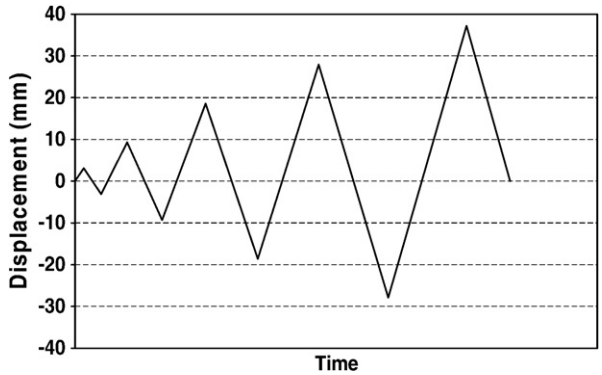

Fig. 7. Time-history of applied displacement on the specimens.

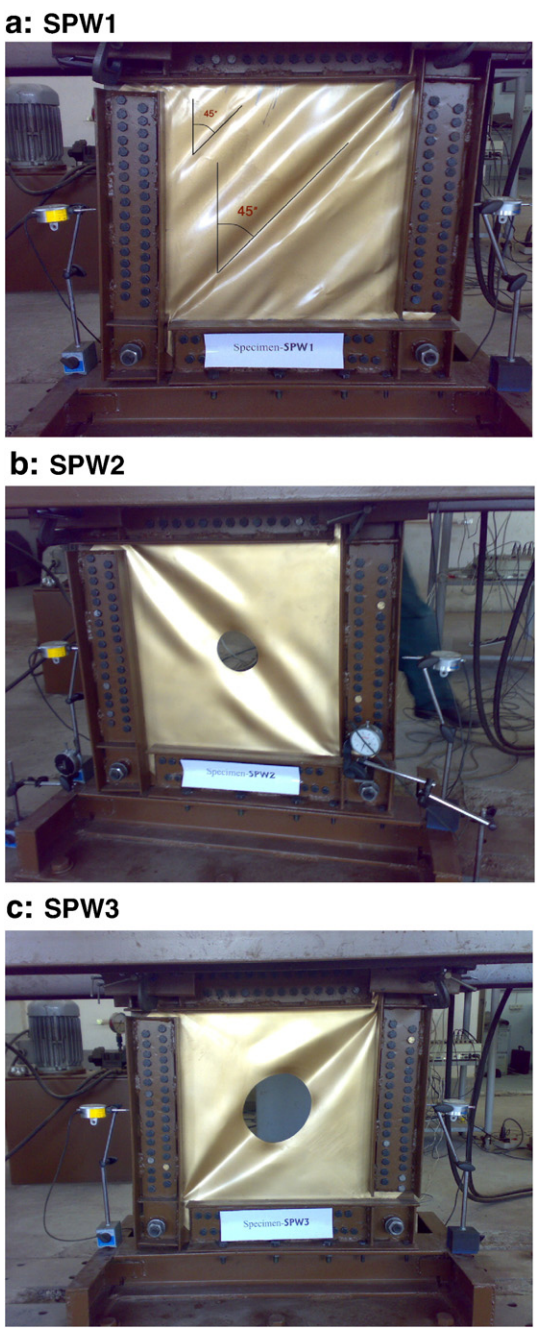

Fig. 8. Deforming and expanding tension field in the experimental specimens.

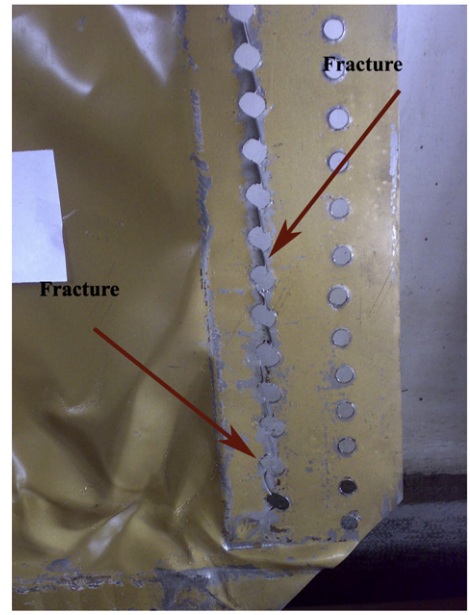

Fig. 9. Bearing failure in the line of bolts in the SPW1 specimen.

frames. This factor is considered in the National Building Code of Canada (NBCC) [13].

$$\text{Ductility Factor } \mu = \frac{\delta_u}{\delta_y} \tag{6}$$

δ_u, according to the definition in the NBCC, is the maximum plastic displacement of the system and can be replaced by δ_{max} (which can be obtained through testing). Because of the dispersed and oscillating results, especially at the beginning of loading, the yielding displacement, δ_y, for calculating the ductility factor was achieved by making the envelope of the hysteresis diagram equivalent to the ideal bilinear diagram of FEMA356 [14] regulated according to item 3.3.3.2.4. The envelope of the hysteresis curve for specimen SPW8 and the relevant ideal bilinear curve are shown in Fig. 13.

By obtaining δ_u and δ_y from test results and setting in Eq. (6), μ can be calculated. The ductility values, along with the failure mode of the experimental specimens, are shown in Table 5. Considering the different failure modes, there is not any possibility for an exact study of the

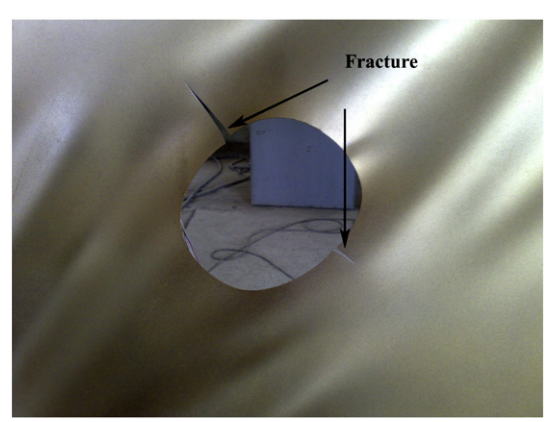

Fig. 10. Failure around the opening because of tension concentration in the SPW6 specimen (drift 3%).

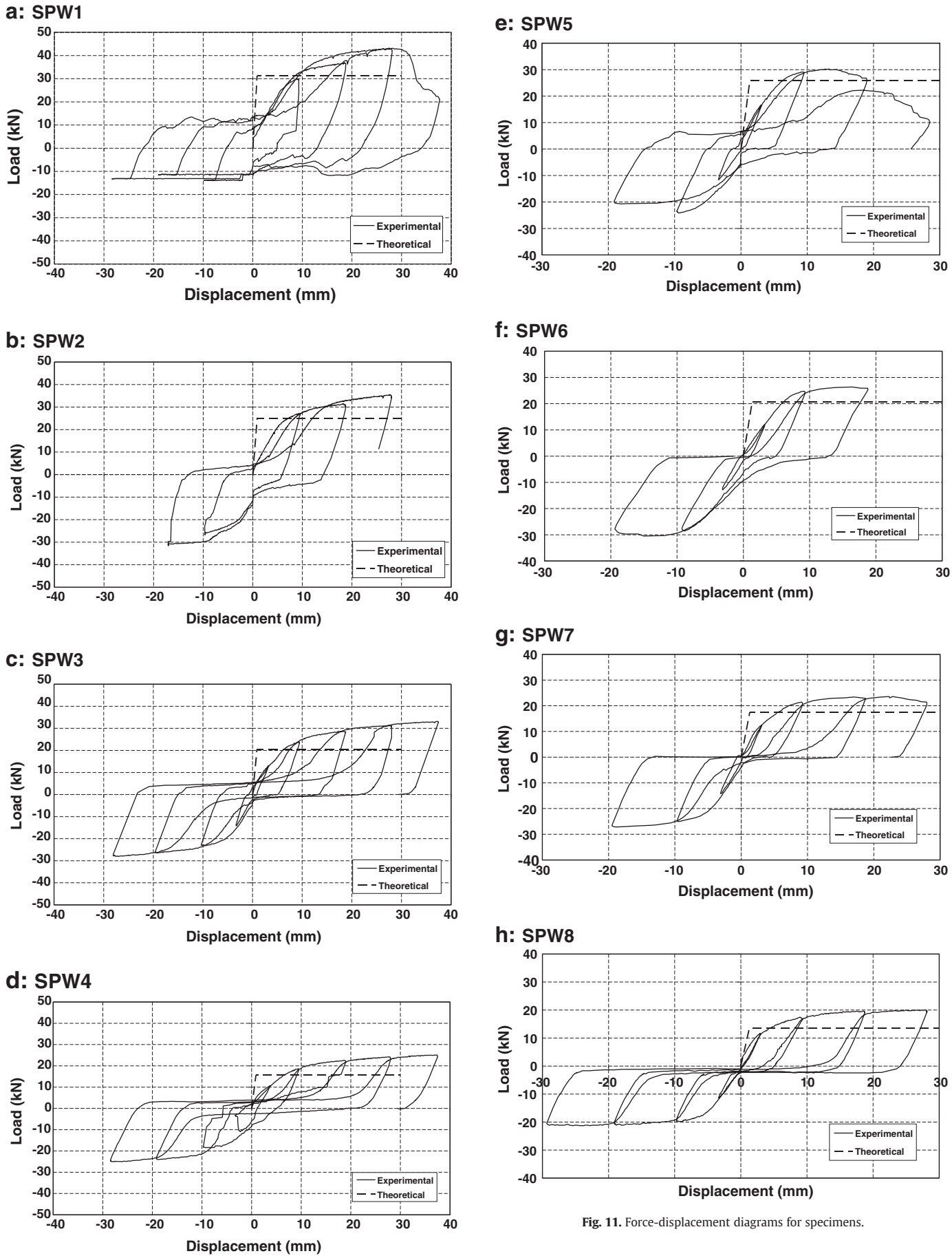

Fig. 11. Force-displacement diagrams for specimens.

Table 3
Summary of experimental and theoretical results.

Specimen	Experimental results					Theoretical results	
	Initial stiffness (kN/mm)	Yielding force (kN)	Pmax+ (kN)	Pmax− (kN)	Energy absorption (kJ)	Initial stiffness* (kN/mm)	Shear strength** (kN)
SPW1	4.5	36.7	42.6	–	4.7	35.0	31.3
SPW2	4.4	27.8	34.8	30.4	1.8	28.4	25.0
SPW3	3.6	26.6	33.1	27.7	2.6	23.1	20.4
SPW4	2.7	20.5	25.0	25.0	1.7	17.8	15.7
SPW5	5.7	26.7	28.7	24.0	1.5	19.3	25.9
SPW6	3.9	25.0	25.9	29.4	0.9	15.5	20.8
SPW7	3.7	23.3	24.6	27.1	1.1	13.6	17.5
SPW8	4.6	16.7	20.1	21.1	1.1	10.5	13.4

* Calculated using Eq. (5)
** Calculated using Eq. (4)

opening dimension effects on the aforementioned parameter; however, on the whole, the ductile behavior of the steel plate shear walls is evident.

4.3. Energy absorption

As it has been shown in the force-displacement diagrams (Fig. 11), the hysteresis loops of the test specimens are in a completely stable S shape with considerable energy absorption characteristics. By increasing the displacement in each cycle, the area under the hysteresis curve increases compared to previous cycles, as shown in Figs. 14 and 15. According to the hysteresis curves for the experimental specimens, it was observed that the plate thickness and the opening dimensions are effective parameters for energy absorption of the system. With an increase in the opening diameter, the pinching effect was more evident and, consequently, the area under the load–displacement diagram decreases. As a result, a decrease in energy absorption takes place.

For studying the effect of the central circular opening on the energy absorption of a steel shear wall, the amounts of dissipated energy in the third cycle of the hysteresis diagrams have been measured, and the percentage of the dissipated energy has been calculated (Table 6).

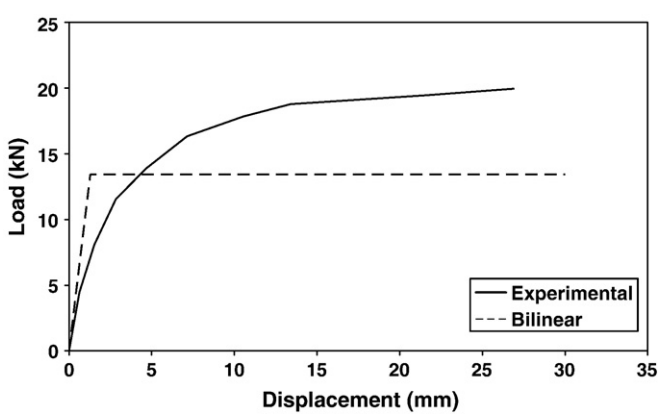

Fig. 12. Comparison of achieved experimental and theoretical results for the SPW8 specimen.

Table 4
Decrease in percent of panel strength with increasing opening dimension.

specimen	SPW1	SPW2	SPW3	SPW4	SPW5	SPW6	SPW7	SPW8
Thickness (mm)	0.7	0.7	0.7	0.7	0.37	0.37	0.37	0.37
Opening ratio	0	0.2	0.35	0.5	0	0.2	0.35	0.5
Decreasing strength (%)	–	14.7	20	38.5	–	2.6	15.0	26.7

As the tension field action and plate yielding were started from the main diagonal, the existence of an opening in the panel center will cause a maximum decrease in energy dissipation. Considering the fact that the reason for energy dissipation is yielding of the steel plate, the decreasing process in the first series of specimens is faster due to eliminating the major amounts of steel in the thicker plates.

4.4. Results of strain gauges

Recorded strain amounts show that, in specimens with openings, the development of the tension field will transfer to secondary diagonals, and a stress concentration was created around the openings. For the SPW4 specimen with 6% drift, the strain in the secondary diagonal St. G5 besides the opening is approximately 10% and along the main diagonal St.G6 is approximately 1.6% (Fig. 16). The locations of the St. G5 and St.G6 strain gauges in the SPW4 specimen are given in Fig. 17. A concentration of stress around the opening in thinner plates and smaller opening diameters will cause plate failure around the opening (Fig. 10).

5. Concluding remarks

The salient concluding tips are as follows. It should be mentioned that the area of these results is limited to the considered conditions for the experimental specimens in this research; however, it is expected that they have more general applications.

- Experimental specimens have a stable S-shaped load–displacement curve regardless of failure mode.
- An opening at the center of the panel will centralize the plate out-of-plane buckling deformations along the main diagonal, and this

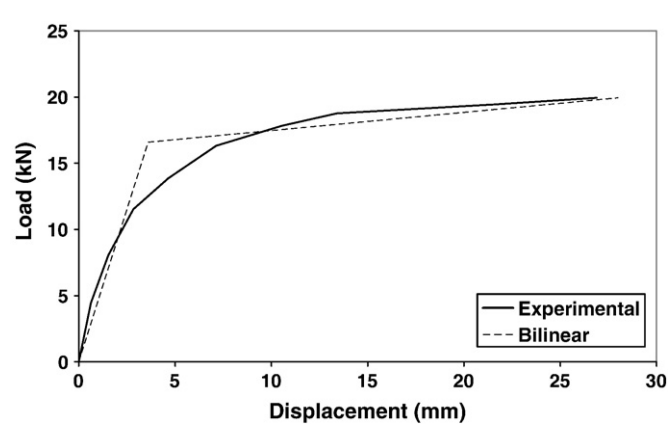

Fig. 13. Hysteresis curve envelope of the experimental specimen SPW8 and the relevant ideal bilinear curve.

Table 5
Ductility values of the experimental specimens.

specimen	SPW1	SPW2	SPW3	SPW4	SPW5	SPW6	SPW7	SPW8
Ductility	3.7	4.5	5.2	5	3.3	3	4.5	7.5
Failure mode	i	ii	iii	iii	i	iv	iv	iii

i: obvious shear and crippling of plate at connection bolts and boundary member locations.
ii: end of test due to energy fluctuation.
iii: complete loading and lack of obvious tear and crippling in plate connection with boundary members and around opening.
iv: observed plate tearing around opening because of stress concentration.

will be more obvious with increasing diameter of the opening. As shown in Fig. 8.

- Despite existing openings with large dimensions, experimental specimens still had high ductility with high energy absorption in loading cycles up to 6% drift with no strength loss except in cases of local failure.
- Specimens without an opening have shown a bearing failure of the plate and bolts in connections, this is due to their higher ultimate strength. But, in perforated specimens with less plate thickness and small openings, plate tearing failure occurred around the opening due to stress concentration; accordingly, an intense loss of strength was seen in the load displacement diagrams.
- The used analytical method has been estimated the ultimate shear strength of the experimental specimens conservatively. But, this method overestimates the initial stiffness because of slippage in bolted connections.

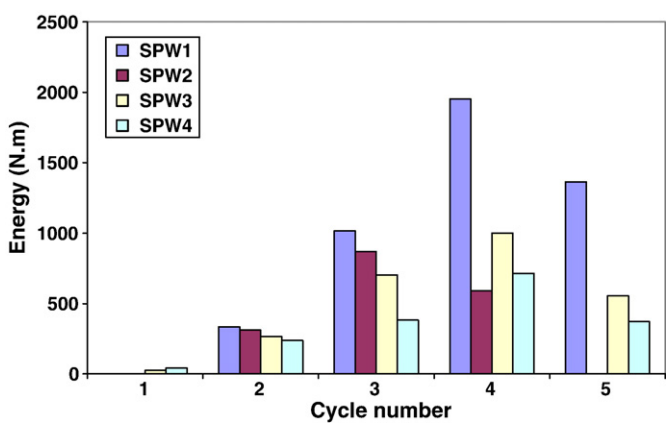

Fig. 14. Absorbed energy in each loading cycle for the first series of specimens.

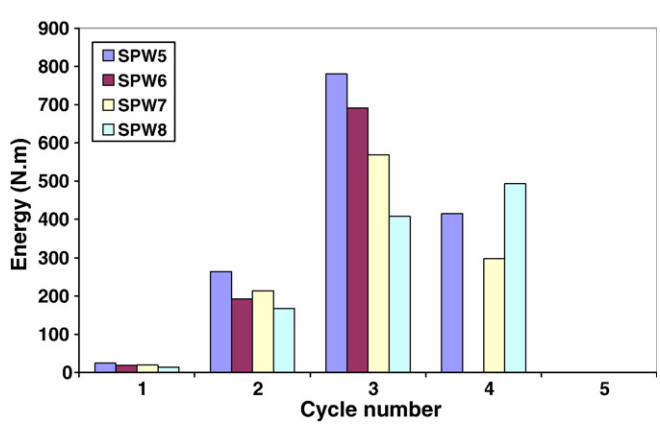

Fig. 15. Absorbed energy in each loading cycle for the second series of specimens.

Table 6
Decrease percentage of absorbed energy by increasing opening diameter.

Specimen	SPW1	SPW2	SPW3	SPW4	SPW5	SPW6	SPW7	SPW8
Thickness (mm)	0.7	0.7	0.7	0.7	0.37	0.37	0.37	0.37
Opening ratio	0	0.2	0.35	0.5	0	0.2	0.35	0.5
Decrease of energy absorption (%)	–	14.5	30.8	62.3	–	11.4	27.1	47.8

- In plates with a thickness of 0.70 mm, the maximum amount of ductility is 5.2, Then, this amount was obtained for a specimen with an opening ratio of 0.35 (SPW3) with a complete loading up to 6% drift and without observing any shear or crippling in the bolted connection between plate and boundary members.
- In plates with a thickness of 0.37 mm, the maximum amount of ductility is 7.5. Then, this amount was obtained for a specimen with an opening ratio of 0.5 (SPW8) with a complete loading up to 4.5% drift and without observing any shear or crippling in the bolted connection between the plate and boundary members.
- Decreasing the plate thickness and increasing the opening diameter was effective in enlarging "pinching" in the load–displacement diagrams. "Pinching" will decrease the area of the hysteresis loops and, as a result, will decrease the energy absorption of the specimens.
- According to the results obtained from the strain gauges, if an opening is created in a steel plate shear wall, a concentration of stress around the opening will happen during the expansion of the plate tension field action. Therefore, the failure mode of the system in specimens with opening diameters of 100 and 175 mm and a thickness of 0.37 mm (SPW6 and SPW7) will be plate failure around the opening as a result of stress concentration around the opening.

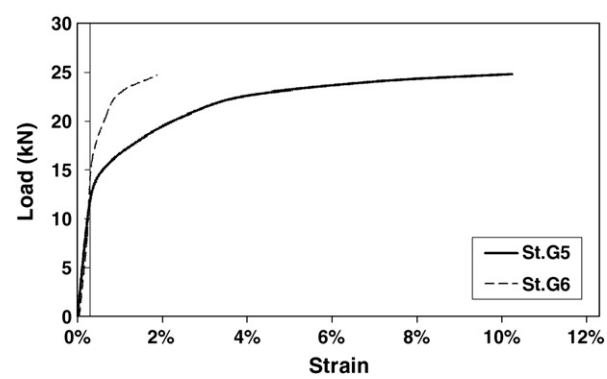

Fig. 16. Strain–load diagram resulted by St.G5 & St.G6 for the SPW4 specimen.

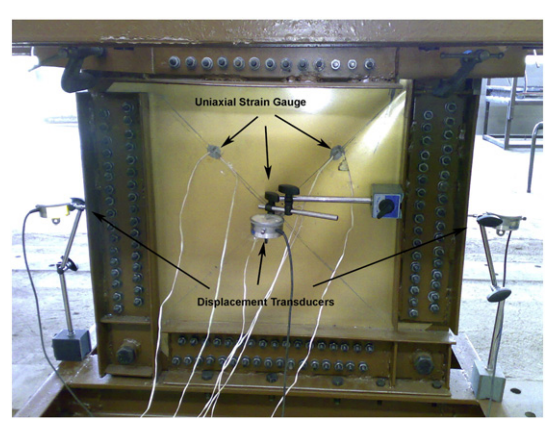

Fig. 17. Location of St.G5 and St.G6 strain gauges on the SPW4 specimen.

References

[1] Kharrazi MHK. Analytical method for analysis and design of steel plate walls," EERF#05-04. Report to Steel Structures Education Foundation (CISC). Vancouver, BC, Canada: Department of Civil Engineering, The University of British Columbia; 2005.
[2] Roberts TM, Sabouri-Ghomi S. Hysteretic characteristics of unstiffened plate shear panels. Thin-Walled Struct 1991;12:145–62.
[3] Roberts TM, Sabouri-Ghomi S. Hysteretic characteristics of unstiffened perforated steel plate shear panels. Thin-Walled Struct 1992;14:139–51.
[4] Deylami A, Daftari H. Non-linear behavior of steel shear wall with large rectangular opening. Proceeding on CD-Rom. 12th World Conference on Earthquake Eng, NewZealand; 2000. Paper No.408.
[5] Vian D, Bruneau M. Testing of special LYS steel plate shear wall. 13th World Conference on Earthquake Eng; 2004. Paper No.978.
[6] ATC-24. Guidelines of cyclic seismic testing on components fo r Steel Structures Applied Technology Council, Redwood City, California, U.S.A; 1992.
[7] Kharrazi MHK, Prion HGL, Ventura Carlos E. Implementation of M-PFI method in design of steel plate walls. J Constr Steel Res 2008;64:465–79.
[8] Timoshenko SP, Gere JM. Theory of elastic stability. Mc Grow-Hill Book Company; 1961.
[9] Valizadeh H. Experimental investigation of seismic behavior of steel shear walls with opening and diagonal stiffeners. MEng thesis, Faculty of Civil Engineering, Urmia University, Urmia, Iran; June 2009.
[10] ASTM. Standard test method and definitions for mechanical testing of steel products, A370/A370-03. American Society for Testing and Materials (ASTM), Philadelphia, PA; 2003.
[11] Elgaaly M. Thin steel plate shear walls behavior and analysis. Thin Walled Struct 1998;32:151–80.
[12] Chan RWK, Albermani F, Wiliams MS. Evaluation of yielding shear panel device for passive energy dissipation. J Constr Steel Res 2009;65:260–8.
[13] National Building Code of Canada. Canadian Commission on Building and Fire Codes. Ottawa, Ontario: National Research Council of Canada; 2005.
[14] FEMA 356, Federal Emergency Management Agency. Prestandard and commentary for the seismic rehabilitation of buildings. American Society of Civil Engineering; 2000.